Molecular cloning and characterization of farnesyl diphosphate synthase from *Rosa rugosa* Thunb associated with salinity stress

Editorial Criteria

Use these criteria points to structure your review. The full detailed editorial criteria is on your [guidance page](#).

BASIC REPORTING

- Clear, unambiguous, professional English language used throughout.
- Intro & background to show context. Literature well referenced & relevant.
- Structure conforms to [PeerJ standards](#), discipline norm, or improved for clarity.
- Figures are relevant, high quality, well labelled & described.
- Raw data supplied (see [PeerJ policy](#)).

EXPERIMENTAL DESIGN

- Original primary research within [Scope of the journal](#).
- Research question well defined, relevant & meaningful. It is stated how the research fills an identified knowledge gap.
- Rigorous investigation performed to a high technical & ethical standard.
- Methods described with sufficient detail & information to replicate.

VALIDITY OF THE FINDINGS

- Impact and novelty not assessed. *Meaningful* replication encouraged where rationale & benefit to literature is clearly stated.
- All underlying data have been provided; they are robust, statistically sound, & controlled.

- Conclusions are well stated, linked to original research question & limited to supporting results.

Molecular cloning and characterization of farnesyl diphosphate synthase from *Rosa rugosa* Thunb associated with salinity stress

Guo Wei [Equal first author, 1] , Yudie Chen [Equal first author, 1] , Jianwen Wang [1] , Liguo Feng [Corresp. 1]

[1] Yangzhou University, Yangzhou, China

Corresponding Author: Liguo Feng
Email address: lgfeng@yzu.edu.cn

Rosa rugosa, a renowned ornamental plant, is cultivated for its essential oil containing valuable monoterpenes, sesquiterpenes, and other compounds widely used in the floriculture industry. Farnesyl diphosphate synthase (FPPS) is a key enzyme involved in the biosynthesis of sesquiterpenes and triterpenes for abiotic or biotic stress. In this study, we successfully cloned and characterized a full-length FPPS- encoding cDNA identified as RrFPPS1 using RT-PCR from *R. rugosa*. Phylogenetic analysis showed that RrFPPS1 belonged to the angiosperm-FPPS clade. Transcriptomic and RT-qPCR analyses revealed that *RrFPPS1* gene had tissue-specific expression patterns. Subcellular localization analysis using *Nicotiana benthamiana* leaves showed that RrFPPS1 was a cytoplasmic protein. *In vitro* enzymatic assays combined with GC-MS analysis showed that RrFPPS1 produced farnesyl diphosphate (FPP) using isopentenyl diphosphate (IPP) and dimethylallyl diphosphate (DMAPP) as substrates to provide a precursor for sesquiterpene and triterpene biosynthesis in the plant. Additionally, our research uncovered that RrFPPS1 was upregulated under salt treatment. These substantially findings contribute to an improved understanding of terpene biosynthesis in *R. rugosa* and open new avenues for advancements in horticultural practices and fragrance industries by overexpression of the *RrFPPS1* gene *in vivo* increased FPP production and subsequently led to elevated sesquiterpene yields in the future. The knowledge gained from this study can potentially lead to the development of enhanced varieties of *R. rugosa* with improved aroma, medicinal properties, and resilience to environmental stressors.

Molecular cloning and characterization of farnesyl
diphosphate synthase from *Rosa rugosa* Thunb
associated with salinity stress

6   Guo Wei*, Yudie Chen*, Jianwen Wang, and Liguo Feng

7   College of Horticulture and Landscape Architecture, Yangzhou University, Yangzhou, China.

8   *These authors contributed equally to this work.

10   Corresponding Author:

11   Liguo Feng

12   Yangzhou University, Yangzhou, Jiangsu, 225009, China

13   Email address: lgfeng@yzu.edu.cn

Abstract

16   *Rosa rugosa*, a renowned ornamental plant, is cultivated for its essential oil containing valuable
17   monoterpenes, sesquiterpenes, and other compounds widely used in the floriculture industry.
18   Farnesyl diphosphate synthase (FPPS) is a key enzyme involved in the biosynthesis of
19   sesquiterpenes and triterpenes for abiotic or biotic stress. In this study, we successfully cloned and
20   characterized a full-length FPPS- encoding cDNA identified as RrFPPS1 using RT-PCR from *R.
21   rugosa*. Phylogenetic analysis showed that RrFPPS1 belonged to the angiosperm-FPPS clade.
22   Transcriptomic and RT-qPCR analyses revealed that *RrFPPS1* gene had tissue-specific expression
23   patterns. Subcellular localization analysis using *Nicotiana benthamiana* leaves showed that
24   RrFPPS1 was a cytoplasmic protein. *In vitro* enzymatic assays combined with GC-MS analysis
25   showed that RrFPPS1 produced farnesyl diphosphate (FPP) using isopentenyl diphosphate (IPP)
26   and dimethylallyl diphosphate (DMAPP) as substrates to provide a precursor for sesquiterpene
27   and triterpene biosynthesis in the plant. Additionally, our research uncovered that RrFPPS1 was
28   upregulated under salt treatment. These substantially findings contribute to an improved
29   understanding of terpene biosynthesis in *R. rugosa* and open new avenues for advancements in
30   horticultural practices and fragrance industries by overexpression of the *RrFPPS1* gene *in vivo*
31   increased FPP production and subsequently led to elevated sesquiterpene yields in the future. The
32   knowledge gained from this study can potentially lead to the development of enhanced varieties
33   of *R. rugosa* with improved aroma, medicinal properties, and resilience to environmental stressors.

34

Introduction

36   Terpenoids are the largest and most diverse groups of natural products, with over 80,000 structures
37   identified to date (Christianson 2017). They play various physiological and ecological roles that

38   are essential for plant growth and development (Dudareva 2007; Zhou & Pichersky 2020) and are
39   involved in various physiological processes such as hormone biosynthesis, photosynthesis,
40   electron transport, and membrane components. Moreover, terpenoids act as important signaling
41   and defense mediators between plants and their environments (Vandermoten et al. 2009). Owing
42   to their remarkable properties, these compounds have significant applications in the food,
43   pharmaceutical, and agricultural industries, making them highly valuable resources (Sarah &
44   Raymond 2004).

45   In plants, terpenoids are synthesized from two independent pathways: the methylerythritol
46   phosphate pathway (MEP) pathway in plastids (Lichtenthaler et al. 1997; Rodriguez-Concepcion
47   & Boronat 2002) and the mevalonate (MVA) pathway in cytosol or peroxisomes (Chen et al. 2011;
48   Sapir-Mir et al. 2008). The MVA-pathway primarily supplies the precursor farnesyl diphosphate
49   (FPP; C_{15}) for the synthesis of sesquiterpenes, triterpenes and sterols (J N Valitova et al. 2016;
50   Natalia et al. 2005). By contrast, the plastidic MEP-pathway provides the precursors such as
51   geranyl diphosphate (GPP; C_{10}), geranylgeranyl diphosphate (GGPP; C_{20}), and geranylfarnesyl
52   diphosphate (GFPP; C_{25}) for the production of monoterpenes, diterpenes, and sesterterpenes,
53   respectively (Chen et al. 2019; Chen et al. 2021; Duilio et al.1997; Huang et al. 2017; Schwender
54   et al. 1997). These reactions are all catalyzed by enzymes commonly referred to as
55   prenyltransferases. Both pathways can provide the terpene building blocks: isopentenyl
56   diphosphate (IPP) and dimethylallyl diphosphate (DMAPP). According to the structure of
57   enzymatic products, these prenyltransferases were grouped into geranyl diphosphate synthase
58   (GPPS), farnesyl diphosphate synthase (FPPS), geranylgeranyl diphosphate synthase (GGPPS)
59   and geranylfarnesyl diphosphate synthase (GFPPS), respectively (Chen et al. 2021; Cui et al. 2022;
60   Song et al. 2023). They function at the branch points of isoprenoid metabolism and thus control
61   IPP and DMAPP flux into different terpenoid families (Kyozo & Tanetoshi 1998).

62   FPPS is a vital enzyme responsible for catalyzing the head-to-tail condensation of IPP and
63   DMAPP to produce FPP (Pichersky & Raguso 2018). Numerous studies investigated the
64   biochemical and molecular biology characteristics of FPPS in a variety of plant species, such as
65   Arabidopsis, rice, maize, *Ginkgo biloba*, *Chimonanthus praecox*, and *Hedychium coronarium*
66   (Cunillera et al. 1997; Kazutsuka et al. 1997; Lan et al. 2013; Chun et al. 1996; Wang et al. 2004;
67   Xiang et al. 2010). In Arabidopsis, the *AtFPPS1* gene is primarily expressed in roots and flowers,
68   and *AtFPPS2* is expressed mainly in flowers (Cunillera et al. 1996). In maize, FPPS1 plays a key
69   role in the biosynthesis of FPP for ubiquinone production, and FPPS2 is primarily responsible for
70   the biosynthesis of isofucosterol. Meanwhile, FPPS3 is closely linked to the production of
71   sesquiterpene volatile (*E*)-*β*-caryophyllene in response to the presence of root-chewing herbivore
72   *Diabrotica virgifera* virgifera (Tang et al. 2022). Despite numerous studies regarding FPPS in
73   various plants, data on FPP formation in *Rosa rugosa* are lacking.

74   *R. rugosa*, native to Eastern Asia, has been cultivated in the floriculture industry worldwide
75   and is renowned for its essential oil extracted from petals, which is used in perfumes, cosmetics,
76   and pharmaceuticals (Bendahmane et al. 2013; Caser & Scariot 2022). *R. rugosa* 'Zi Zhi' is a
77   continuously flowering variety that offers significant possibilities for yielding more essential oil

78   (Bai et al. 2021). The essential oil of *R. rugosa* mainly consists of monoterpenes, sesquiterpenes
79   and other valuable compounds (Ueyama et al. 1990). Despite significant knowledge about
80   monoterpene biosynthesis, the molecular mechanisms of sesquiterpene biosynthesis in *R. rugosa*
81   remain poorly understood. Given that FPPS plays a pivotal role in generating FPP, a critical
82   precursor for sesquiterpene biosynthesis, unraveling the mechanisms of FPPS formation enhances
83   our understanding of the essential oil production in *R. rugosa*. Plant growth and development are
84   often influenced by environmental stresses, with salinity stress being one of the most severe
85   challenges (Zhu 2001). Although FPPS is closely associated with terpenoid production, studies
86   examining the effect of abiotic stress on FPPS, particularly in *R. rugosa*, are limited (Tian et al.
87   2018).
88   In this study, we aimed to identify potential FPPS from *R. rugosa*. A comprehensive
89   characterization of the identified FPPS was then conducted to provide insight into the molecular
90   mechanism of FPP formation. We also investigated whether the FPPS from *R. rugosa* exhibits any
91   response to salt stress. Using a combination of bioinformatics, transcriptomic, molecular, and
92   biochemical approaches, we successfully identify a FPPS as the key enzyme responsible for FPP
93   formation. Our findings address a gap in the molecular mechanism of sesquiterpene biosynthesis
94   in *R. rugosa*.
95

96   ## Materials & Methods
97   ### Plant Materials
98   Plant materials were collected from the resource nursery of Yangzhou University (32.391°N,
99   119.419°E), Yangzhou, China. The leaves and flowers of 3-year-old cutting seedlings of *R. rugosa*
100   'ZiZhi' were collected for further analysis (May/2022). The samples were immediately frozen in
101   liquid nitrogen and then stored at − 80 °C for RNA extraction.
102

103   ### RNA Extraction and Gene Expression Analysis
104   Total RNA was extracted from the collected plant tissues using the TaKaRa MiniBEST Plant RNA
105   Extraction Kit (TaKaRa) as per the manufacturer's instructions. The concentration and quality of
106   the total RNA were evaluated through NanoDrop 1000 analysis and gel electrophoresis. For
107   reverse transcription, first-strand cDNA was synthesized from the total RNA using a
108   PrimeScript™ II 1st Strand cDNA Synthesis Kit (Takara) following the manufacturer's protocol.
109   RT-qPCR analysis was performed with HiScript III RT SuperMix for qPCR (Vazyme) as per the
110   manufacturer's instructions.
111   The expression levels of RrFPPS in roots (OR: roots of open-air and TR: roots of tissue
112   culture seedlings), branches (PB, SB, and TB represent the primary, secondary, and tertiary lateral
113   branches, respectively) and flowers (S1–S7 represent the seven flower stages, respectively. S1,
114   small bud stage; S2, large bud stage; S3, reddish stage; S4, flowering initiation stage; S5, initial
115   opening stage; S6, semi-opening stage; S7, full opening stage) were analyzed by reverse
116   transcription quantitative real-time PCR (RT-qPCR) and using the previous transcriptomic data
117   (Wang et al. 2022) of *R. rugosa* 'Zi Zhi' providing the per kilobase of exon model per million

118 mapped fragments (FPKM) of *RrFPPSs*. ChamQ SYBR qPCR Master Mix (Vazyme) was used
119 for RT-qPCR on a CFX96 real-time PCR platform (Bio-Rad). The internal control gene was *5.8S*
120 *rRNA*. The primers for *RrFPPS* and the internal control gene were designed using the Genscript
121 online website (https://www.genscript.com) and synthesized by Tsingke Biotech (Beijing). The
122 primer sequences are provided in the supplementary file (Supplementary Table 1).
123 A 20 µL reaction mixture containing 1 µL of cDNA template, 10 µM of the primers, and 10
124 µL of 2×ChamQ SYBR qPCR Master Mix used in accordance with the manufacturer's
125 instructions. Reactions were performed with an initial incubation at 95 °C for 30 s, followed by 39
126 cycles at 95 °C for 10 s and 60 °C for 30 s. Three independent biological replicates with three
127 technical replicates were prepared for each sample. The relative transcript levels of *RrFPPSs* in
128 different tissues were calculated using the $2^{-\triangle\triangle Ct}$ method (Livak & Schmittgen 2001) based on
129 the threshold cycle (Ct) values generated from the CFX Manager software from Bio-Rad
130 (https://www.bio-rad.com/sites/default/files/webroot/web/pdf/lsr/literature/10014295.pdf).   All
131 the experiments were carried out at least in triplicate. Values were analyzed by ANOVA using
132 Graphpad Prism (http://www.graphpad.com/faq/viewfaq.cfm?faq=1362mega). *P*-values less than
133 0.05 were considered significant.
134

In-Silico Analysis of RrFPPS and Phylogenetic Analysis

136 Possible FPPS genes were searched using a well-characterized *Arabidopsis thaliana* FPPS
137 (AAB07248.1) protein involved in the isoprenoid biosynthesis pathway as a query through
138 BLASTP with the genome of *R. rugosa* 'Zi Zhi' (unpublished) (Cunillera et al. 1996). Candidate
139 genes were further confirmed by Pfam (http://pfam.xfam.org/) and the Conserved Domain
140 Database. The physicochemical properties of RrFPPS were analyzed using the ProtParam tool
141 from the online software Expasy (https://web.expasy.org/protparam/). Multiple alignments of
142 amino acid sequences were conducted with CLUSTALX and GENEDOC. Multiple sequence
143 alignment of *RrFPPS* sequences and the construction of a phylogenetic tree, were achieved using
144 the neighbor-joining method of MEGA X software (substitution type: amino acid and *p*-distance
145 model) (Kumar et al. 2018). Bootstrapping was performed by resampling from the 1000 replicates.
146 Protein sequences used for alignment were as follows: *R. chinensis* G/FPPS1 (A0A2P6Q231), *R.*
147 *chinensis* FPPS2 (A0A2P6QLH7), *Fragaria vesca* FPPS (XP_004294906), *Malus domestica*
148 FPPS (AAM08927), *Centella asiatica* FPPS (AAV58896), *Lupinus albus* FPPS (P49351),
149 *Humulus lupulus* FPPS (BAB40665), *Panax ginseng* FPPS (AAY87903), *Prunus persica* FPPS
150 (XP_007211529), *Vitis vinifera* FPPS (AAX76910), *Potentilla anserina* FPPS (XP_050367607),
151 *Hevea brasiliensis* FPPS (AAM98379), *Artemisia annua* FPPS (AAD17204), *Salvia miltiorrhiza*
152 FPPS (AEZ55677), *Paeonia lactiflora* FPPS (AKJ26301), *Jasminum sambac* FPPS
153 (AIY24422),*Ginkgo biloba* FPPS (AAR27053), and *Picea abies* FPPS (ACA21460).The
154 GenBank accessions and protein sequences of FPPS are shown in Supplementary Table 2.
155

Isolation and Cloning of the RrFPPS Coding Sequence

157 The open reading frame (ORF) of RrFPPS was amplified using PrimeSTAR Max DNA
158 Polymerase (Takara) and PCR primers designed with NEB Tm Calculator
159 (https://tmcalculator.neb.com/). Reverse-transcribed cDNA served as the PCR template. The PCR
160 products were purified using the FastPure Gel DNA Extraction Mini Kit (Vazyme), cloned into
161 pEASY-Blunt cloning vectors (TransGen Biotech), and transformed into *Escherichia coli* Trans1-
162 T1 (TransGen Biotech) competent cells. The PCR-positive clones were selected and sequenced by
163 Sangon Biotech (Shanghai, China). The sequence information of RrFPPS is shown in
164 Supplementary Table 2.
165

Subcellular Localization of RrFPPS Proteins

167 The subcellular localization of RrFPPS was predicted using the bioinformatics analysis website
168 WoLF PSORT (https://wolfpsort.hgc.jp/). The ORF of RrFPPS was amplified with specific
169 primers, and inserted into the pCAMBIA 1300-35S-sGFP vector using the ClonExpress II One
170 Step Cloning Kit (Vazyme) with Sac1/Xba1 restriction enzymes. The constructs and the empty
171 vector (control) were transformed into Agrobacterium tumefaciens strain GV3101+P19 by the
172 freezethaw method. Single positive Agrobacterium clones were grown in Luria-Bertani (LB)
173 medium until the OD_{600} reached 0.5-0.6 and then infiltrated into 5 to 6 week-old *Nicotiana*
174 *benthamiana* leaves. The fluorescence of the tobacco plant leaves was examined 2 days after
175 infiltration at 488 nm using an LSM 880 confocal microscope (Zeiss) to obtain images of the GFP
176 fluorescence signal.
177

Purification of Recombinant RrFPPS Proteins and Enzymatic Assay

179 For enzymatic assays, RrFPPS was cloned downstream of the (His)6-tag sequences in pEasy Blunt
180 E1 plasmids to express RrFPPS-His recombinant proteins. The constructed vectors were verified
181 through DNA sequencing and transformed into chemically competent *E. coli* BL21 (DE3) pLysS
182 cells (Transgen). Single positive colonies were selected and grown in LB medium containing
183 ampicillin (100 μg/mL) at 37 °C in a shaking incubator until the OD_{600} of the culture reached 0.4-
184 0.6. Afterward, 0.4 mM isopropyl β-D-thiogalactopyranoside (IPTG) was added, and the culture
185 was incubated at 16 °C and 200 rpm for 12 h to induce the recombinant proteins. The induced cells
186 were collected by centrifugation at 5,000 g for 10 min and stored at − 80 °C.
187 The cells were resuspended in binding buffer (20 mM Tris-HCl, 500 mM NaCl, 10% glycerol,
188 10 mM imidazole, and 0.5 mM phenylmethylsulfonyl fluoride (PMSF), pH 7.5) and sonicated to
189 disrupt them. The lysate was centrifuged at 12,000 rpm for 30 min at 4 °C, and Ni- nickel-
190 nitrilotriacetic acid (NTA) agarose (Sangon Biotech) was added to the supernatant for affinity
191 purification following the manufacturer's instructions. The protein was added to the desalting
192 buffer (250 mM MOPS, 100 mM $MgCl_2$, 50% glycerol (1:1, vol:vol), pH 7.5) to obtain desalted
193 protein, which was then applied to a Sephadex Desalting Gravity Column (Sangon Biotech) in
194 accordance with the manufacturer's instructions.
195 Enzymatic activity assays were performed using gas chromatography–mass spectrometry
196 (GC–MS), in a final volume of 100 μL reaction volume containing 66 μM IPP, 44 μM DMAPP,

197   10 μL desalted enzyme solution, and ddH$_2$O up to 100 μL to determine the *in vitro* activity of
198   RrFPPS. After incubation at 30 °C for 2 h, the assay mixture was hydrolyzed overnight at 30 °C
199   using 1 unit of calf intestinal alkaline phosphatase (CIP) and 1 unit of apyrase from potatoes. The
200   volatile products were adsorbed by Headspace solid-phase microextraction using 30 μm
201   (CAR/PDMS layer) and 50 μm (DVB layer) (Supelco Inc., Bellefonte, PA) overnight. The volatile
202   compounds were collected from headspace and subjected to GC–MS (Clarus SQ8T, PerkinElmer,
203   USA). The experimental procedure involved initial heating to 50 °C and holding it for 1 min, then
204   increasing to 120 °C at 5 °C min^{-1}, 200 °C at 8 °C min^{-1}, and 250 °C at 12 °C min^{-1} for 7 min.
205   The mass spectrometry (MS) conditions included the emission current of 200 μA, ionization
206   energy of 70 eV, and mass scan range of 29-600 amu.

207

Quantification of the Transcript Levels of *RrFPPS* Genes under Salt Treatment

and the roots?

210   One-month-old *R. rugosa* plants were treated with 100 mM NaCl solution for 1 h, and their leaves
211   were collected with three biological repetitions. Another three plants soaked in deionized water
212   for 1 h were set as the control group (CK). The leaves of salt treatment and CK plants (three
213   replications for each) were picked, immediately frozen with liquid nitrogen, and stored at −80°C.
214   For RNA isolation, and cDNA synthesis, the cDNA of salt treatment and control was used as the
215   template for SYBR green PCR amplification to examine the RrFPPS expression pattern. ChamQ
216   SYBR qPCR Master Mix (Vazyme) was used for RT-qPCR on a CFX96 real-time PCR platform
217   (Bio-Rad), and the reactions were performed as previously reported (Livak & Schmittgen 2001).
218   Three independent biological replicates with three technical replicates were prepared for each
219   sample. The relative transcript levels of RrFPPSs in different treatments were calculated using the
220   $2^{-\triangle\triangle Ct}$ method (Livak & Schmittgen 2001) based on the threshold cycle (Ct) values generated
221   from the CFX Manager software (from Bio-Rad). The values were analyzed as previously
222   mentioned.

223

Results

Identification of *RrFPPS* Genes in *R. rugosa* Genome

and what?

226   To investigate terpene biosynthesis in *R. rugosa*, particularly terpenes derived from FPP. Analysis
227   revealed two potential full-length *FPPS* genes designated as RrFPPS1 and RrFPPS2
228   (Rru05G067530 and Rru05G000330). The full-length cDNA sequence of RrFPPS1 measured
229   1153 bp, including an 82 bp 5'-untranslated region and a 42 bp 3'-untranslated region. Meanwhile,
230   the full-length cDNA sequence of RrFPPS2 was 1449 bp, comprising a 104 bp 5'-untranslated
231   region and a 316 bp 3'-untranslated region. The ORFs of RrFPPS1 and RrFPPS2 were each 1029
232   bp in length, encoding a protein of 342 amino acids. The predicted molecular mass of the RrFPPS1
233   protein was 39.57 kDa with a theoretical pI of 5.39. Similarly, the predicted molecular mass of the
234   RrFPPS2 protein was 39.42 kDa with a theoretical pI of 5.52.
235   Sequence alignment analysis of RrFPPS protein sequences with other plant FPPS proteins

236 revealed the presence of five highly conserved regions (I-V) that are essential for substrate binding
237 and catalytic activityand typically seen in prenyltransferases (Fig 1). These regions comprise the
238 substrate binding pocket, substrate-Mg^{2+} binding site, catalytic site, and two aspartate-rich regions,
239 namely, Asp-rich motif 1 and 2. The first is first Asp-rich motif (FARM) in region II, with the
240 sequence $DD_{XX(2-4)}D$ (D = aspartic acid and X = any amino acid), and the second is second Asp-
241 rich motif (SARM) in region V with the sequence $DD_{XX}D$.
242 To investigate the evolutionary relationships between RrFPPS and FPPS proteins from other
243 species, we selected typical FPPS proteins from *R. chinensis, Arabidopsis thaliana, F. vesca, M.*
244 *domestica, C. asiatica, P. ginseng, P. persica,* and *Potentilla ansering,* and constructed a
245 phylogenetic tree. Phylogenetic analysis revealed that despite the high sequence homology, all
246 plant FPPSs were separated into two major clades: clade of angiosperm. Our analysis showed that
247 RrFPPS have high homologous to FPPSs from other species. RrFPPS1 and RrFPPS2 appeared to
248 fall in two separate subclades. Given that RrFPPS2 showed 100% identity to RcG/FPPS1(*R.*
249 *chinensis*), we focused on the biochemical function of RrFPPS1 hereafter (Fig 2).
250

Tissue Expression Profiling of the *RrFPPS* Genes

252 To investigate the tissue-specific expression patterns of RrFPPS in *R. rugosa*, both transcriptomic
253 analysis and RT-qPCR were used to evaluate and quantify transcript levels. Transcriptomic
254 analysis showed that a high transcript of RrFPPS2 was detected in all tissues, and a high transcript
255 of RrFFPPS1 was detected in S7 of the flower. In flowers, the expression level of RrFPPS2 was
256 higher than that of RrFPPS1. Both genes had increased expression from S1 to S7, reaching the
257 maximum level at the S7 stage. Moreover, RrFPPS2 had the highest transcript in branches (Fig
258 3A). RT-qPCR results of leaves and flowers from 3-year-old cutting seedlings also revealed that
259 RrFPPS1 and RrFPPS2 were similarly expressed in two tissues but with distinct expression
260 patterns. Both genes showed higher relative expression levels in flowers than in leaves (Fig 3B).
261

Subcellular Localization of the RrFPPS Proteins

263 FPP is commonly synthesized through the cytosolic MVA pathway (Chen et al. 2011; Sapir-Mir
264 et al. 2008). To investigate the subcellular localization of RrFPPSs, we expressed them in
265 *N.benthamiana* leaves. The results indicated that RrFPPS1 and RrFPPS2 were localized in the
266 cytosol (Fig 4). These findings support the notion that RrFPPS1 is responsible for producing FPP
267 in the cytosol, which is then used in the biosynthesis of FPP-derived compounds.
268

Functional Characterization of the Recombinant RrFPPS1

270 Inspired by the discovery of the bifunctionality of RcG/FPPS1 from *R. chinensis*, which produces
271 GPP and FPP in the cytosolic MVA pathway, we investigated the function of RrFPPS1. To
272 elucidate the role of RrFPPS1, we expressed and purified the recombinant protein in *E. coli* using
273 Ni-NTA chromatography. The RrFPPS1 protein was subjected to *in vitro* enzyme activity assays
274 using DMAPP and IPP as substrates. GC-MS for product analysis conclusively demonstrated that
275 the function of RrFPPS1 as a fully functional FPP synthase (Fig 5).

Expression Analysis of *RrFPPS* Genes under Salt Treatment

Terpenoids play crucial ecological roles in plant environment interactions. To investigate how *R. rugosa* responds to salt stress, we exposed *R. rugosa* plants to salt treatment and examined the expression levels of RrFPPS1 and RrFPPS2 using RT-qPCR. Our findings revealed a significant increase in the mRNA levels of RrFPPS1 and RrFPPS2 in *R. rugosa* leaves under salt treatments. This observation suggested a potential defensive role for these genes in response to salt-induced stress (Fig 6).

Discussion

This study comprehensively investigated the terpene biosynthesis in *R. rugosa*, focusing on FPP biosynthesis. The results led to the identification of RrFPPSs in *R. rugosa* 'Zi Zhi' genome (unpublished data), representing a significant achievement in understanding the terpene biosynthetic pathway in this plant species. Tissue expression profiling revealed that RrFPPS1 was expressed in all tissues with distinct expression patterns. Subcellular localization of RrFPPS1 revealed that it is a cytosolic protein, and the phylogenetic analysis showed that RrFPPS1 is similar to RcFPPS2 (*R. chinensis*), suggesting potential functional similarities between these enzymes (Conart et al. 2023). Further examinations, such as biochemical assays or structural analysis, are warranted to reveal their biochemical functions in each species.

Although a number of FPPSs have been characterized from angiosperms and gymnosperms, the identification of RrFPPS1 is a significant achievement because FPPS is a key enzyme involved in terpene biosynthesis in *R. rugosa*. The FARM and SARM regions are suggested to function as binding sites for the diphosphate moieties of IPP and allylic substrates (Kartika & Anil 1996) (Fig 1). The presence of conserved regions (FARM and SARM), which are typical of prenyltransferases, in RrFPPS1 indicated that these proteins are functionally active and may play a crucial role in FPPS-derived terpene biosynthesis in *R. rugosa*. The FARM in domain II plays a role in the determination of chain length for the resulting prenyl pyrophosphates in the presence of a conserved Phe residue located five amino acids upstream of the DDxxD motif. The SARM in domain V is the binding site for the homoallylic substrate IPP (Ohnuma et al. 1996). Therefore, the conservation of these regions suggested that RrFPPS may share a similar mechanism of substrate binding and catalysis with other plant FPPS enzymes. However, this finding must be validated by biochemical experiments or structural similarity analysis. Phylogenetic analysis revealed that RrFPPS1 is highly similar to RcFPPS2 and falls into the angiosperm clade. The FPPS enzymes in gymnosperms may primarily contribute to metabolites such as sterols, which are also derived from FPP, while in angiosperms, apart from participating in primary metabolism, FPPs are likely to be involved in the volatile compounds found in flowers and belong to secondary metabolites (Weng et al. 2021). These findings suggested that RrFPPS1 shares a close genetic relationship with other FPPSs within the Rosaceae family, indicating the conserved function of FPPS in Rosaceae family.

316 Tissue expression profiling of RrFPPS in *R. rugosa* provided valuable insights into the tissue-
317 specific expression patterns of RrFPPS1. A preferential accumulation of RrFPPS1 mRNAs was
318 observed in lateral branches, followed by flowers and roots. The significantly higher expression
319 levels of RrFPPS1 in flowers compared with that in leaves suggested its essential role in the
320 biosynthesis of terpenes, which are known to contribute to the enchanting flower scent that is
321 characteristic of roses. Our study and the recent research by Conart et al. (2023), suggested that
322 although RrFPPS1 plays a more dominant role in plant primary metabolism, RrFPPS2 is more
323 involved in floral scent biosynthesis (Weng et al. 2021). These findings indicated that RrFPPS1
324 possibly has an important role in the biosynthesis of other terpenoids, such as terpene alcohols,
325 sterols, ubiquinone, photosynthetic pigments, and plant hormones, all of which are essential for
326 plant growth, development, and immunity (Degenhardt et al. 2009). Furthermore, our study
327 indicated that the expression of two *RrFPPS* genes significantly responded to salt treatment. We
328 propose that the upregulation of the *RrFPPS* genes can lead to an increase in FPP substrate
329 availability for sesquiterpenoid and/or triterpenoid biosynthesis, which could aid in coping with
330 challenging environments (Teuber et al. 2008). These findings underscored the ecological
331 importance of RrFPPSs in *R. rugosa*'s adaptation to its habitat.
332 Functional characterization of the recombinant RrFPPS1 protein revealed that it can produce
333 FPP from IPP and DMAPP substrates, indicating that it is functionally active and plays a crucial
334 role in the synthesis of important secondary metabolites. In particular, sesquiterpenes, are
335 responsible for imparting pungent or aromatic flavors to specific plant tissues and are released in
336 response to wounding and insect attack (Rosenkranz et al. 2021). In roses, sesquiterpenes have
337 been traditionally used as flavors and fragrances and possess various biological properties, such as
338 anticancer and antimalarial activities (Zhou et al. 2020).
339 Despite the progress made in this study, its limitations must be acknowledged. For fully
340 elucidating the specific roles and functions of *RrFPPS*1 gene, virus-induced gene silencing (VIGS)
341 or CRISPR-Cas9 techniques may be necessary to precisely manipulate *RrFPPS1* expression.
342 These approaches would provide comprehensive insights into *R. rugosa*. With this additional
343 information at our disposal, we can enhance our comprehension of the mechanisms governing
344 terpene biosynthesis and potentially explore novel targets for genetic modification or breeding
345 programs in the future.
346

Conclusions

348 The cloned and characterized of FPPSs from *R. rugosa* reported in this study are involved in
349 terpene biosynthesis. The relative expression of RrFPPS1 was the highest in the flowers, and that
350 of RrFPPS2 was the highest in the branch. Subcellular localization analysis revealed that RrFPPS1
351 and RrFPPS2 were cytoplasmic. Our work fills a gap in the understanding of the molecular
352 mechanisms involved in sesquiterpene biosynthesis in *R. rugosa* and its function response to salt
353 stress. The findings opened up new avenues for the overexpression of the native *FPPS* gene into
354 *R. rugosa*.
355

356

Acknowledgements

358 All authors thank the anonymous reviewers and editors for their valuable comments and
359 suggestions. *you're welcome :)*

360

Funding

362 The study was funded by the National Natural Science Foundation of China (Grant No. 32372738
363 and 32171861), and the Natural Science Foundation of Jiangsu Province (BK20231331). The
364 funders had no role in study design, data collection and analysis, decision to publish, or preparation
365 of the manuscript.

366

Competing Interests

368 The authors declare that they have no competing interests.

369

AUTHOR CONTRIBUTION:

371 • Guo Wei conceived and designed the experiments, authored or reviewed drafts of the article,
372   and approved the final draft.
373 • Yudie Chen performed the experiments, analyzed the data, prepared figures and/or tables,
374   authored drafts of the article, and approved the final draft.
375 • Jianwen Wang analyzed the data and approved the final draft.
376 • Liguo Feng conceived and designed the experiments, authored or reviewed drafts of the
377   article, and approved the final draft.

378

Data Availability

380 The following information was supplied regarding data availability: The raw data are available in
381 the Supplemental File.

382

383

384

385

386

387

388

389

390

391

392

393

394

395

396

397

References

399 Bai M, Liu J, Fan C, Chen Y, Chen H, Lu J, Sun J, Ning G, Wang C. 2021. KSN heterozygosity is
400   associated with continuous flowering of *Rosa rugosa* Purple branch. *Horticulture*
401   *Research* 8(26) DOI 10.1038/s41438-021-00464-8.
402 Bendahmane M, Dubois A, Raymond O, Bris ML. 2013. Genetics and genomicsof flower initiation
403   and development in roses. *Journal of Experimental*
404   *Botany* 64:847-857 DOI 10.1093/jxb/ers387.
405 Caser M, Scariot V. 2022. The contribution of volatile organic compounds (VOCs) emitted by
406   petals and pollen to the scent of garden roses. *Horticulturae* 8(11)
407   DOI 10.3390/horticulturae8111049.
408 Chen F, Tholl D, Bohlmann J, Pichersky E. 2011. The family of terpene synthases in plants: a
409   mid-size family of genes for specialized metabolism that is highly diversified throughout
410   the kingdom. *Plant Journal* 66:212-229
411   DOI 10.1111/j.1365-313X.2011.04520.x.
412 Chen Q, Jiang T, Liu Y, Liu H, Zhao T, Liu Z, Gan X, Hallab A, Wang X, He J, Ma Y, Zhang F, Jin
413   T, Schranz ME, Wang Y, Bai Y, Wang G. 2019. Recently duplicated sesterterpene (C25)
414   gene clusters in *Arabidopsis thaliana* modulate root microbiota. *Science China Life*
415   *Sciences* 62:947-958 DOI 10.1007/s11427-019-9521-2.
416 Chen Q, Li J, Ma Y, Yuan W, Zhang P, Wang G. 2021. Occurrence and biosynthesis of plant
417   sesterterpenes (C25), a new addition to terpene diversity. *Plant Communications* 2(5)
418   DOI 10.1016/j.xplc.2021.100184.
419 Christianson DW. 2017. Structural and chemical biology of terpenoid cyclases. *Chemical Reviews*
420   117:11570-11648 DOI 10.1021/acs.chemrev.7b00287.
421 Conart C, Bomzan DP, Huang XQ, Bassard JE, Paramita SN, Saint-Marcoux D,Rius-Bony A,
422   Hivert G, Anchisi A, Schaller H, Hamama L, Magnard JL, Lipko A, Swiezewska E, Jame
423   P, Riveill G, Hibrand-Saint Oyant L, Rohmer M, Lewinsohn E, Dudareva N, Baudino S,
424   Caissard JC, Boachon B. 2023. A cytosolic bifunctional geranyl/farnesyl diphosphate
425   synthase provides MVA-derived GPP for geraniol biosynthesis in rose flowers. *Proc Natl*
426   *Acad Sci USA* 120(19)
427   DOI 10.1073/pnas.2221440120.
428 Chun Ping Li, Brian A. Larkins. 1996. Identification of a maize endosperm-specific cDNA encoding
429   farnesyl pyrophosphate synthetase. *Gene* 171:193-196
430   DOI 10.1016/0378-1119(95)00880-2.
431 Cui B, Zhao X, Chen G, Qin S, Liu Y, Han Z, Yan Q, Han L, Liu S, Liu S, Liu H. 2022. Functional
432   analysis of two terpene synthase genes isolated from the flowers of Hosta 'So Sweet'.
433   *Horticulturae* 8(5) DOI 10.3390/horticulturae8050447.
434 Cunillera N, Arró M, Delourme D, Karst F, Boronat A, Ferrer A. 1996. *Arabidopsis thaliana*
435   contains two differentially expressed farnesyl-diphosphate synthase genes. *Journal of*
436   *Biological Chemistry* 271:7774-7780
437   DOI 10.1074/jbc.271.13.7774.
438 Cunillera N, Boronat A, Ferrer A. 1997. The *Arabidopsis thaliana FPS1* gene generates a novel
439   mRNA that encodes a mitochondrial farnesyl-diphosphate synthase isoform. *Journal of*
440   *Biological Chemistry* 272:15381-15388
441   DOI 10.1074/jbc.272.24.15381.

442 Degenhardt J, Kollner TG, Gershenzon J. 2009. Monoterpene and sesquiterpene synthases and
443   the origin of terpene skeletal diversity in plants. *Phytochemistry* 70:1621-1637
444   DOI 10.1016/j.phytochem.2009.07.030.
445 Dudareva JGN. 2007. The function of terpene natural products in the natural world. *Nature*
446   *Chemical Biology* 3:408-411 DOI 10.1038/nchembio.2007.5.
447 Duilio Arigoni, Silvia Sagner, Christoph Latzel, Wolfgang Eisenreich, Adelbert Bacher, and
448   Meinhart H. Zenk. 1997. Terpenoid biosynthesis from 1-deoxy-D-xylulose in higher
449   plantsby intramolecular skeletal rearrangement. *Proc Natl Acad Sci USA* 94:10600–10605
450   DOI 10.1073/pnas.94.20.10600.
451 Huang AC, Kautsar SA, Hong YJ, Medema MH, Bond AD, Tantillo DJ, Osbourn A. 2017.
452   Unearthing a sesterterpene biosynthetic repertoire in the Brassicaceae through genome
453   mining reveals convergent evolution. *Proceedings of the National Academy of Sciences*
454   114 DOI 10.1073/pnas.1705567114.
455 J N Valitova, A G Sulkarnayeva, F V Minibayeva. 2016. Plant sterols: Diversity, biosynthesis, and
456   physiological functions. *Biochemistry* 81(8):819-834
457   DOI 10.1134/S0006297916080046.
458 Kartika Adiwilaga, Anil Kush. 1996. Cloning and characterization of cDNA encoding farnesyl
459   diphosphate synthase from rubber tree (*Hevea brasiliensis*). *Plant Molecular Biology*
460   30:935-946
461   DOI 10.1007/BF00020805.
462 Kazutsuka Sanmiya, Toshisuke Iwasaki, Makoto Matsuoka, Mitsue Miyao, Naoki Yamamoto.
463   1997. Cloning of a cDNA that encodes farnesyl diphosphate synthase and the blue-light-
464   induced expression of the corresponding gene in the leaves of rice plants. *Biochimica et*
465   *Biophysica Acta* 1350:240-246 DOI 10.1016/s0167-4781(96)00231-x.
466 Kyozo Ogura, Tanetoshi Koyama. 1998. Enzymatic aspects of isoprenoid chain elongation Kyozo.
467   *Chemical Reviews* 98:1263-1276 DOI 10.1021/cr9600464.
468 Kumar S, Stecher G, Li M, Knyaz C, Tamura K. 2018. MEGA X: Molecular evolutionary genetics
469   analysis across computing platforms. *Molecular Biology and Evolution* 35:1547-1549.
470   10.1093/molbev/msy096.
471 Lan JB, Yu RC, Yu YY, Fan YP. 2013. Molecular cloning and expression of Hedychiumcoronarium
472   farnesyl pyrophosphate synthase gene and its possible involvement in the biosynthesis of
473   floral and wounding/herbivory induced leaf volatile sesquiterpenoids. *Gene* 518:360-367
474   DOI 10.1016/j.gene.2013.01.007.
475 Lichtenthaler HK, Schwender J, Disch A, Rohmer M. 1997. Biosynthesis of isoprenoids in higher
476   plant chloroplasts proceeds via a mevalonate-independent pathway. *FEBS Lett* 400:271-
477   274 DOI 10.1016/s0014-5793(96)01404-4.
478 Livak K J, Schmittgen T D. 2001. Analysis of relative gene expression data using real-time
479   quantitative PCR and the $2^{-\triangle\triangle C_T}$ Method. Methods 25:402-408
480   DOI 10.1006/meth.2001.1262.
481 Natalia Dudareva SA, Irina Orlova, Nathalie Gatto, Michael Reichelt, David Rhodes,Wilhelm
482   Boland, Jonathan Gershenzon. 2005. The nonmevalonate pathway supports
483   bothmonoterpene and sesquiterpene formationin snapdragon flowers. *Proc Natl Acad Sci*
484   *USA* 102:933-938 DOI 10.1073/pnas.0407360102.
485 Ohnuma S, Hirooka K, Hemmi H, Ishida C, Ohto C, Nishino T. 1996. Conversion of product
486   specificity of archaebacterial geranylgeranyl-diphosphate synthase. Identification of
487   essential amino acid residues for chain length determination of prenyltransferase reaction.
488   *Journal of Biological Chemistry* 271:18831-18837
489   DOI 10.1074/jbc.271.31.18831.
490 Pichersky E, Raguso RA. 2018. Why do plants produce so many terpenoid compounds? *New*
491   *Phytologist* 220:692-702 DOI 10.1111/nph.14178.
492 Rodriguez-Concepcion M, Boronat A. 2002. Elucidation of the methylerythritol phosphate

493   pathway for isoprenoid biosynthesis in bacteria and plastids. A metabolic milestone
494   achieved through genomics. *Plant Physiology* 130:1079-1089 DOI 10.1104/pp.007138.
495 Rosenkranz M, Chen Y, Zhu P, and Vlot AC. 2021. Volatile terpenes - mediators of plant-to-plant
496   communication. *Plant Journal* 108:617-631
497   DOI 10.1111/tpj.15453.
498 Sapir-Mir M, Mett A, Belausov E, Tal-Meshulam S, Frydman A, Gidoni D, Eyal Y. 2008.
499   Peroxisomal localization of Arabidopsis isopentenyl diphosphate isomerases suggests
500   that part of the plant isoprenoid mevalonic acid pathway is compartmentalized to
501   peroxisomes. *Plant Physiology* 148:1219-1228
502   DOI 10.1104/pp.108.127951.
503 Sarah A Holstein, Raymond J Hohl. 2004. Isoprenoids: Remarkable diversity of form and functio.
504   *Lipids* 39:293–309 DOI 10.1007/s11745-004-1233-3.
505 Schwender J, Zeidler J, Groner R, Muller C, Focke M, Braun S, Lichtenthaler FW, Lichtenthaler
506   HK. 1997. Incorporation of 1-deoxy-D-xylulose into isoprene and phytol by higher plants
507   and algae. *FEBS Lett* 414:129-134 DOI 10.1016/s0014-5793(97)01002-8.
508 Song S, Jin R, Chen Y, He S, Li K, Tang Q, Wang Q, Wang L, Kong M, Dudareva N, Smith BJ,
509   Zhou F, Lu S. 2023. The functional evolution of architecturally different plant geranyl
510   diphosphate synthases from geranylgeranyl diphosphate synthase. *The Plant Cell*
511   35:2293-2315 DOI 10.1093/plcell/koad083.
512 Tang HV, Berryman DL, Mendoza J, Yactayo-Chang JP, Li QB, Christensen SA, Hunter CT, Best
513   N, Soubeyrand E, Akhtar TA, Basset GJ, Block AK. 2022. Dedicated farnesyl diphosphate
514   synthases circumvent isoprenoid-derived growth-defense tradeoffs in *Zea mays*. *Plant
515   Journal* 112:207-220 DOI 10.1111/tpj.15941.
516 Teuber M, Zimmer I, Kreuzwieser J, Ache P, Polle A, Rennenberg H, Schnitzler JP. 2008. VOC
517   emissions of Grey poplar leaves as affected by salt stress and different N sources. *Plant
518   Biology* 10:86-96
519   DOI 10.1111/j.1438-8677.2007.00015.x.
520 Tian X, Wang Z, Zhang Q, Ci H, Wang P, Yu L, Jia G. 2018. Genome-wide transcriptome analysis
521   of the salt stress tolerance mechanism in *Rosa chinensis*. *PLoS One* 13:e0200938
522   DOI 10.1371/journal.pone.0200938.
523 Ueyama Y, Hashimoto S, Nii H, Furukawa K. 1990. The essential oil from the flowers of *Rosa
524   rugosa* Thunb. var.plena Regel. *Flavour and Fragrance Journal* 5:219-222
525   DOI 10.1002/ffj.2730050406.
526 Vandermoten S, Haubruge E, Cusson M. 2009. New insights into short-chain prenyltransferases:
527   structural features, evolutionary history and potential for selective inhibition. *Cell Mol Life
528   Sci* 66:3685-3695 DOI 10.1007/s00018-009-0100-9.
529 Wang P, Liao Z, Guo L, Li W, Chen M, Pi Y, Gong Y, Sun X, Tang K. 2004. Cloning and functional
530   analysis of a cDNA encoding *Ginkgo biloba* farnesyl diphosphate synthase. *Molecules
531   and Cells* 18:150-156.
532 Weng JK, Lynch JH, Matos JO, Dudareva N. 2021. Adaptive mechanisms of plant specialized
533   metabolism connecting chemistry to function. *Nature Chemical Biology* 17:1037-1045
534   DOI 10.1038/s41589-021-00822-6.
535 Xiang L, Zhao K, Chen L. 2010. Molecular cloning and expression of *Chimonanthus praecox*
536   farnesyl pyrophosphate synthase gene and its possible involvement in the biosynthesis of
537   floral volatile sesquiterpenoids. *Plant Physiology and Biochemistry* 48:845-850
538   DOI 10.1016/j.plaphy.2010.08.015.
539 Zhou F, Pichersky E. 2020. More is better: the diversity of terpene metabolism in plants. *Current
540   Opinion in Plant Biology* 55:1-10 DOI 10.1016/j.pbi.2020.01.005.
541 Zhou L, Yu C, Cheng B, Wan H, Luo L, Pan H, Zhang Q. 2020. Volatile compound analysis and
542   aroma evaluation of tea-scented roses in China. *Industrial Crops and Products* 155
543   DOI 10.1016/j.indcrop.2020.112735.

544   Zhu J. 2001. Plant salt tolerance. *TRENDS in Plant Science* 6:66-71 0.1016/s1360-
545   1385(00)01838-0.

Figure 1

Sequence alignment of the deduced amino acid of *R. rugosa* FPPS and FPPSs from other plants.

FvFPPS, *Fragaria vesca*; MdFPPS, *Malus domestica*; CaFPPS, *Centella asiatica*; HlFPPS, *Humulus lupulus*; OsFPPS, *Oryza sativa*; RcG/FPPS, *Rosa chinensis*; RrFPPS, *Rosa rugosa*. This alignment was shaded using Genedoc software to show conserved amino acid residues in dark blue and similar residues in pink and blue with the similarity of 75% and more than 50% respectively. The five conserved domains of prenyltransferases are boxed and marked by Roman numerals (I-V), which are the substrate binding pocket, aspartate-rich regions 1, catalytic site, substrate-Mg^{2+} binding site and aspartate-rich regions 2. The highly conserved first and second aspartate rich regions (DD$_{XX(2-4)}$D) is presented in domains II and V.

Figure 2

Phylogenetic tree of the amino acid sequences of FPPS from various organisms.

The numbers in the figure represent the genetic distance. Bootstrap values are shown as a percentage of 1000 replicates. RrFPPS1 and RrFPPS2 are marked by red dots. The scale bar on the bottom-left is representative of the degree of difference among sequences where in a distance of 0.05 infers a 5% difference among sequences.

scientific name:
italic or

Rosa rugosa FPPS2
Rosa chinensis G/FPPS1
Potentilla anserina FPPS
Malus domestica FPPS
Prunus persica FPPS
Arabidopsis thaliana FPPS
Paeonia lactiflora FPPS
Jasminum sambac FPPS
Lupinus albus FPPS
Hevea brasiliensis FPPS
Rosa rugosa FPPS1
Rosa chinensis FPPS2
Fragaria vesca FPPS
Artemisia annua FPPS
Centella asiatica FPPS
Panax ginseng FPPS
Humulus lupulus FPPS
Santalum album FPPS
Vitis vinifera FPPS

Angiosperm

Picea abies FPPS
Ginkgo biloba FPPS

Gymnosperms

0.05

Figure 3

Analysis of gene expression of RrFPPS1 and RrFPPS2.

Fig.3A Gene expression profiles in the roots, lateral branches, and flowers of *R. rugosa* 'Zi Zhi'. A heat map was generated based on the normalized Log2 FPKM represented by the blue-yellow gradation. The numbers in the heat map were FPKM from RNA-seq data. The OR and TR columns represent the roots of open-air and tissue culture seedlings, respectively. The columns of FB, SB, and TB represent the primary, secondary, and tertiary lateral branches, respectively. The columns of S1–S7 represent the seven flower stages, respectively. **Fig.3B** Gene expression of RrFPPS1 and RrFPPS2 in the flower and leaf of *R. rugosa* 'Zi Zhi' obtain with RT-qPCR. RrFPPS1 and RrFPPS2 expression values were normalized to the levels of *5.8S RNA* expression in respective stage. Data presented are $2^{-\Delta\Delta Ct}$ levels calculated relative to the special tissue. Data are presented as mean ± SE, n = 3.

A
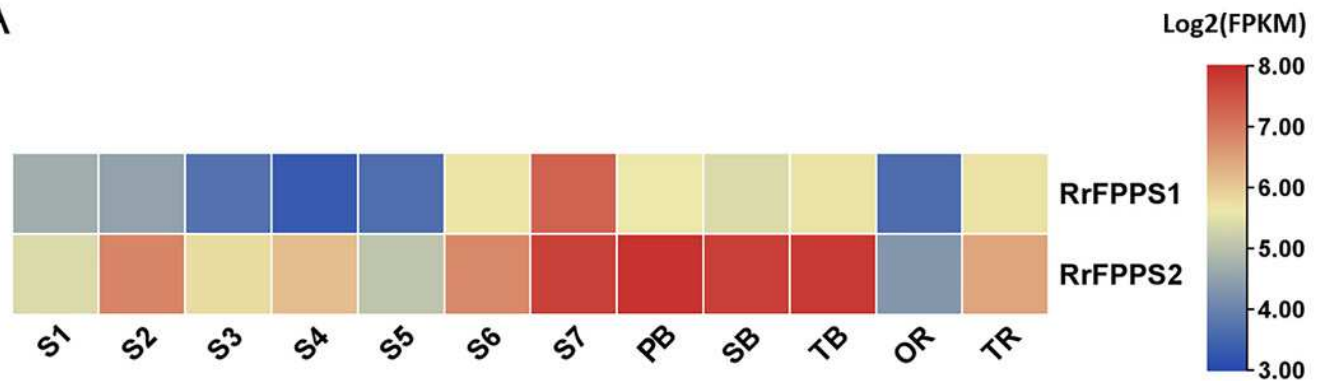
B
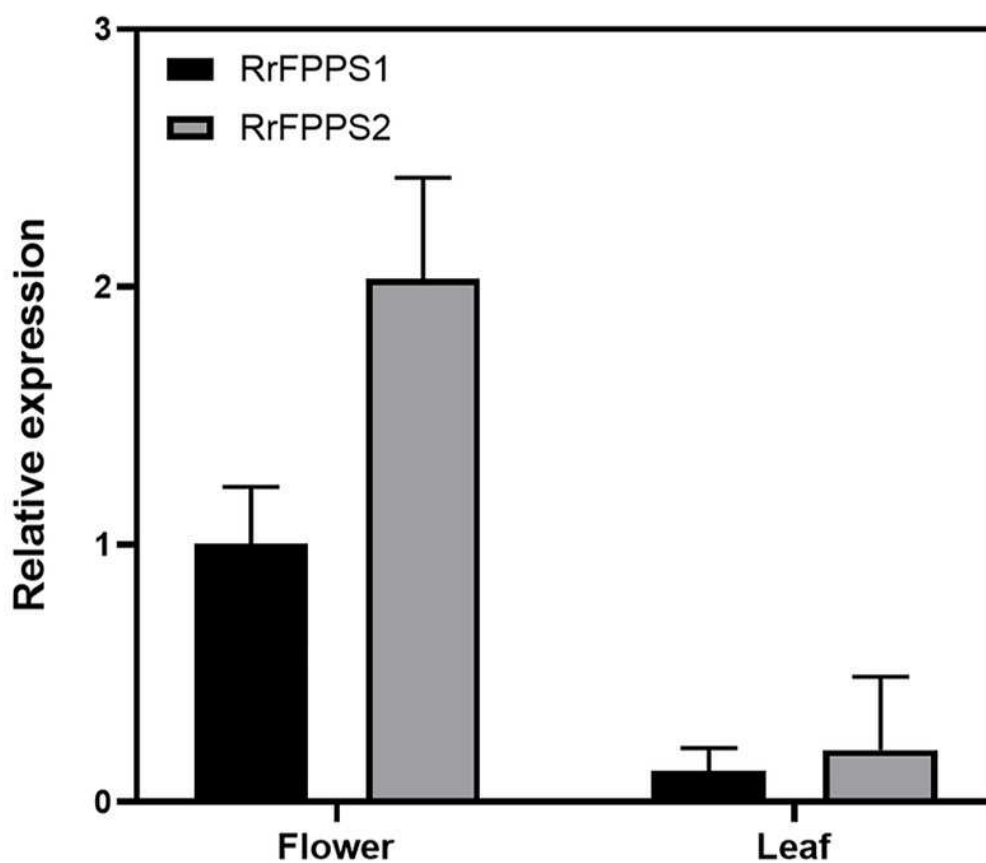
Figure 4

Subcellular localization of RrFPPS1 and RrFPPS2 in the *N. benthamiana* leaves.

GFP (green fluorescent protein) signals from the adaxial leaf surface were observed by using a confocal laser scanning microscope. 'GFP' showed the green signal of the RrFPPSs–GFP fusion proteins or control (the GFP protein was expressed by the pCAMBIA1300-cGFP empty vector as control); 'Autofluorescence' showed the red autofluorescence of chlorophyll; 'Merge' showed the overlay of GFP and autofluorescence and 'Bright field' showed the bright field photograph.
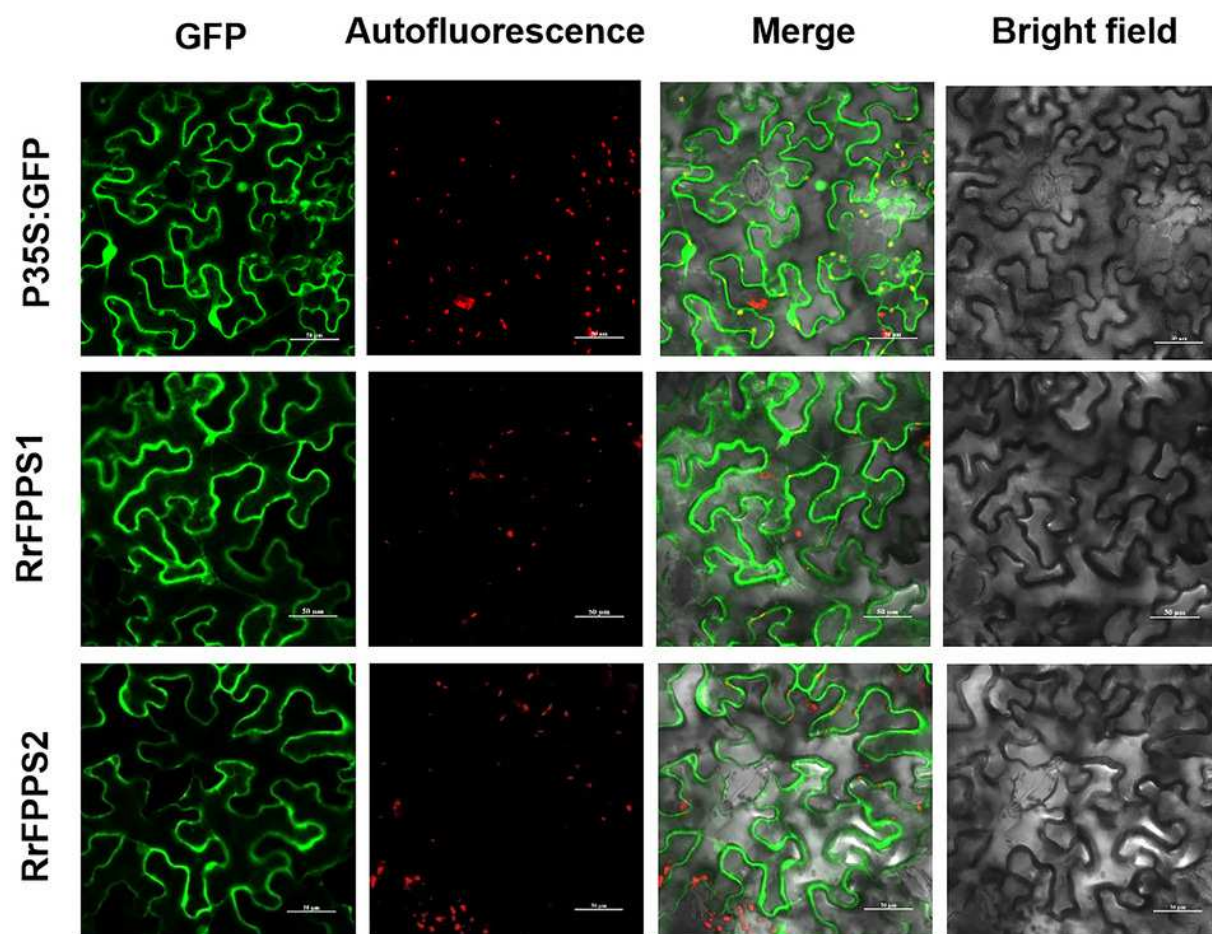
Figure 5

GC-MS analysis of the reaction products catalyzed by purified recombinant RrFPPS1 incubated with IPP and DMAPP.

Fig.5A The reaction products catalyzed by recombinant RrFPPS1 using IPP and DMAPP as substrates.

Fig.5B The mass spectrogram of the reaction products catalyzed by recombinant RrFPPS1.
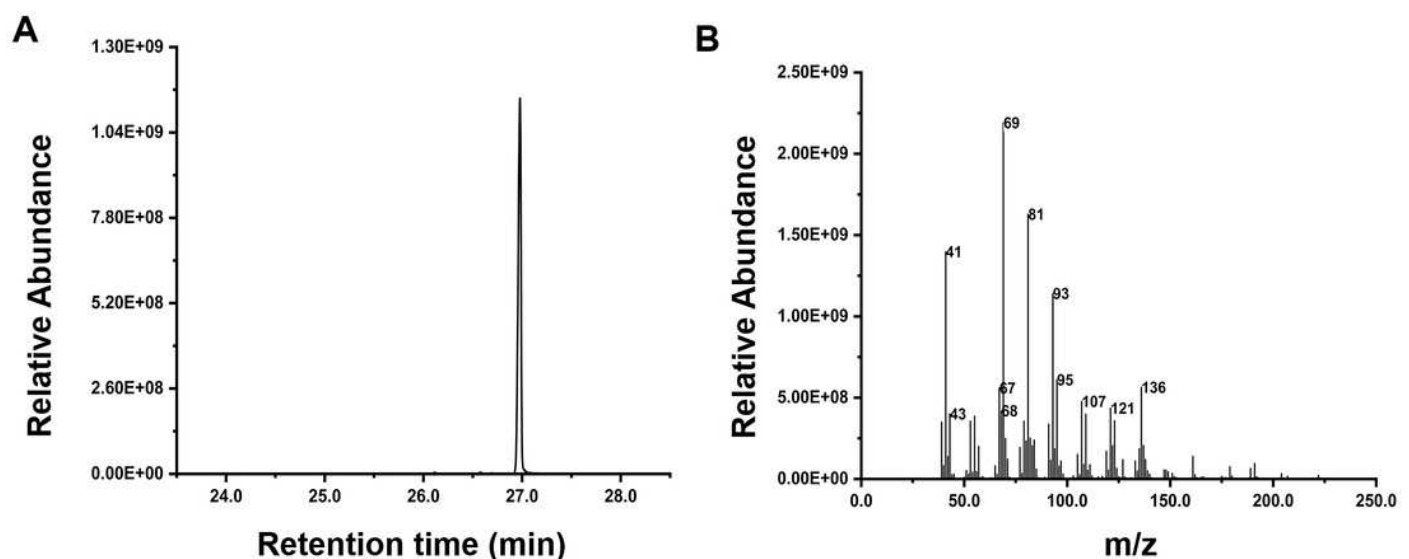
Figure 6

Change fold in *RrFPPSs* RNA levels in response to salt treatment

Expression changes of the RrFPPSs gene were determined in *R. rugosa* treated with salt in comparison with that in control cultures after the initiation of treatment: 1 h. Data are presented as mean ± SE, n = 3. Asterisks indicate statistically significant differences (t-test : *, $P < 0.05$; **, $P < 0.01$).